Topological transformation of a trefoil knot into a [2]catenane

Thirumurugan Prakasam[1], Rana Bilbeisi [2], Roberto El-Khoury[1], Loïc J. Charbonnière,[3] Mourad Elhabiri,[4] Gennaro Esposito,[1,5] John-Carl Olsen[6] and Ali Trabolsi[1]*

[1]New York University Abu Dhabi (NYUAD), Experimental Research Building, Building C1, Saadiyat Island, Abu Dhabi, UAE

[2]American University of Beirut, Department of Civil and Environmental Engineering (CEE), Faculty of Engineering and Architecture (FEA), Beirut, Lebanon

[3] Laboratoire d'Ingénierie Moléculaire Appliquée à l'Analyse, IPHC UMR 7178 CNRS-Université de Strasbourg, ECPM, 25 rue Becquerel, 67087 Strasbourg, France

[4] Laboratoire de Chimie Bioorganique et Médicinale, UMR 7509 CNRS-Université de Strasbourg, ECPM, 25 rue Becquerel, 67087 Strasbourg, France

[5] DMIF, Udine University, 33100 Udine, Italy

[6] Department of Chemistry, RC Box 270216, University of Rochester, Rochester, NY, 14627

Supporting Information

Table of Contents

1. General materials and methods

All reagents and starting materials were purchased from Sigma-Aldrich and used without further purification. The zinc(II)-templated trefoil knot (**Zn-TK**) and the cadmium(II)-templated trefoil knot (**Cd-TK**) were synthesized as previously reported.[1, 2] Thin-layer chromatography (TLC) was performed on silica gel 60 F254 (E. Merck). The plates were inspected with UV light. Column chromatography was performed on silica gel 60F (Merck 9385, 0.040–0.063 mm). Routine nuclear magnetic resonance (NMR) spectra were recorded at 25 °C on a Bruker Avance III spectrometer, with working frequencies of 600 and 500 MHz for ^1H, and 151.0 and 125.0 MHz for ^{13}C nuclei. All chemical shifts are reported in ppm relative to the signals corresponding to the residual non-deuterated solvents (CD_3CN: $\delta = 1.94$ ppm, CD_3OD: $\delta = 3.31$ ppm) and deuterated water was calibrated using an internal standard 1% TMS.[3] All ^{13}C spectra were recorded with the simultaneous decoupling of proton nuclei. Coupling constant values (*J*) are given in hertz (Hz). The multiplicity of the proton spectrum is abbreviated in the following way: s (singlet), d (doublet), dd (doublet of doublets), t (triplet), q (quartet), qt (quintet), sx (sextet), m (multiplet) and a wide signal is preceded by br (broad). High resolution mass spectrometry (HRMS) was performed using an Agilent 6540 UHA Accurate Mass Q-TOF / LC - MS-spectrometer in the positive mode and an acetonitrile/water gradient was used with a C-18 column.

2. Transformation of Zn-TK into Zn-[2]C

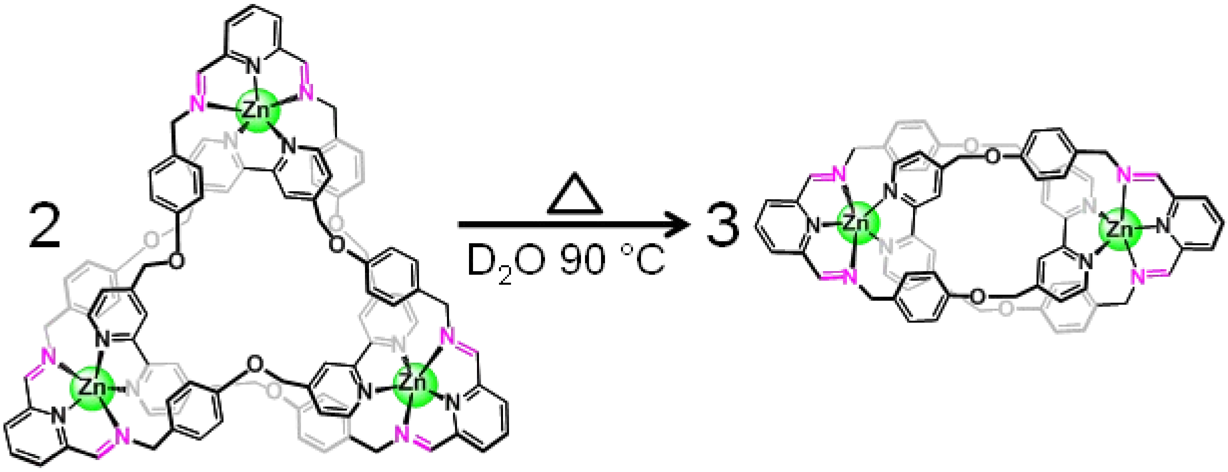

Zn-TK•6CF$_3$CO$_2^-$ **Zn-[2]C**•4CF$_3$CO$_2^-$

Deuterated water (D$_2$O) solutions (0.85 mM, 1.7 mM and 3.4 mM) of the zinc-containing trefoil knot were placed in an NMR tube and heated (conventionally) to 90 ºC. The progress of the reaction was monitored by ^{1}H NMR spectroscopy at room temperature and regular time intervals. After reaction completion, **Zn-[2]C** was precipitated upon addition of a mixed solvent of isopropanol and THF (2:1). The precipitate was washed four times with the hot solvent mixture to remove side-products, including open chain zinc complexes which were estimated to amount to less than 10 mol % of the total product mixture. The final precipitate was dried under vacuum for 4h and characterized by ^{1}H and ^{13}C NMR spectroscopy and HRMS.

Zn-[2]C: Yield: 89 %. ^{1}H NMR (500MHz, D$_2$O, 25 °C): δ 5.03 (s, 8H, Ar-CH_2), 5.43 (s, 8H, Ar-CH_2), 6.60 (ABq, 16H, J = 12 Hz, Ar-H), 7.97 (d, 4H, J = 4.5 Hz, Ar-H), 8.10 (s, 4H, Ar-H), 8.37 (s, br, 4H, Ar-H), 8.64 (d, 4H, J = 8.2 Hz, Ar-H), 8.94 (t, 2H, J = 7.8 Hz, Ar-H), 9.16 (s, 4H, Ar-H); ^{13}C NMR (75 MHz, MeOD-d$_4$, 25 °C): δ 63.6, 68.3, 116.6, 117.7 (q, $^2J_{C\text{-}F}$ = 255 Hz, TFA), 122.1, 127.0, 128.0, 129.7, 130.1, 131.0, 135.4, 148.4, 148.8, 148.9, 152.9, 158.4, 161.7 (q, $^3J_{C\text{-}F}$ = 34.5 Hz. TFA); MS (ESI-HRMS): m/z Calcd for $(C_{70}H_{58}F_6N_{10}O_8Zn_2)^{2+}$: 704.146 [M–2TFA]$^{2+}$, found: 704.147 [M–2TFA]$^{2+}$, m/z Calcd for $(C_{68}H_{58}F_3N_{10}O_6Zn_2)^{3+}$: 431.769 [M–3TFA]$^{3+}$, found: 431.768 [M–3TFA]$^{3+}$.

Monitoring the H_h and H_j protons of Zn-[2]C

The ***h*** and ***j*** protons of **Zn-TK** and **Zn-[2]C** were monitored in order to follow the evolution of the interconversion process. The mole-percent formation of each topological structure was deduced from the integrals of its corresponding protons and by using the rough approximation that the two structures were the only ones present. Origin 7.0 was used to fit a kinetic model to the data, with the assumption that the interconversion involves a single rate limiting step, *i.e.* that the concentration of each species varied in a mono-exponential fashion over time: $\%_{\mathbf{Zn\text{-}[2]C}} = p1 + p2 \times \exp(-p3 \times t)$ with $p1$ = mole % of **Zn-[2]C** at t = 0 s, $p2$ = mole % **Zn-[2]C**, $p3$ = apparent first order rate constant, k_{obs}, in s^{-1} and t the time in s. $p1$ was fixed at 0 because the experiments started with pure **Zn-TK** in D_2O and $p2$ is close to 100% in most cases, which indicates that after sufficient time the process is quantitative.

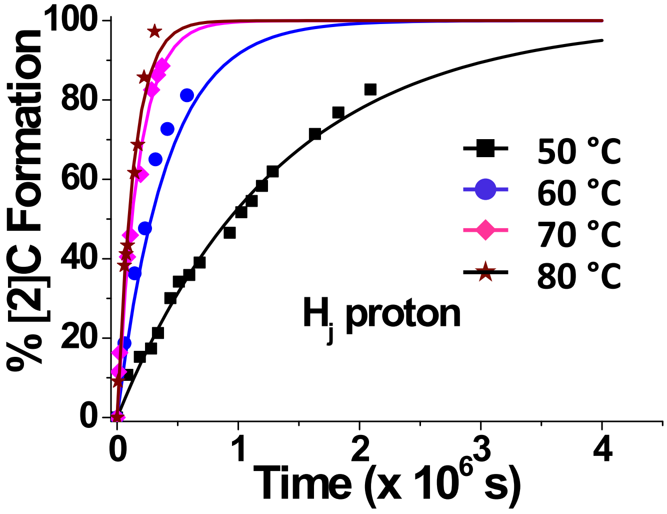

50 °C $k_{obs} = 0.75(2) \times 10^{-6}\ s^{-1}$
60 °C $k_{obs} = 3.07(8) \times 10^{-6}\ s^{-1}$
70 °C $k_{obs} = 5.70(3) \times 10^{-6}\ s^{-1}$
80 °C $k_{obs} = 7.30(4) \times 10^{-6}\ s^{-1}$

Figure S1: Relative population of **Zn-[2]C** plotted against reaction time. Intensities of the H_j NMR proton signals of **Zn-TK** and **Zn-[2]C** were used to determine percent formation of **Zn-**

[2]C. Four samples, each 1.7 mM solutions of **Zn-TK** in D_2O were heated to four different temperatures: 50, 60, 70, or 80 °C. Solid lines in the plot represent the best fits for a first order kinetic process. k_{obs} values are presented in the box at the right. [2]C decomposed at the higher temperatures, which prevented the reaction from being monitored for as long as it was at 50 °C.

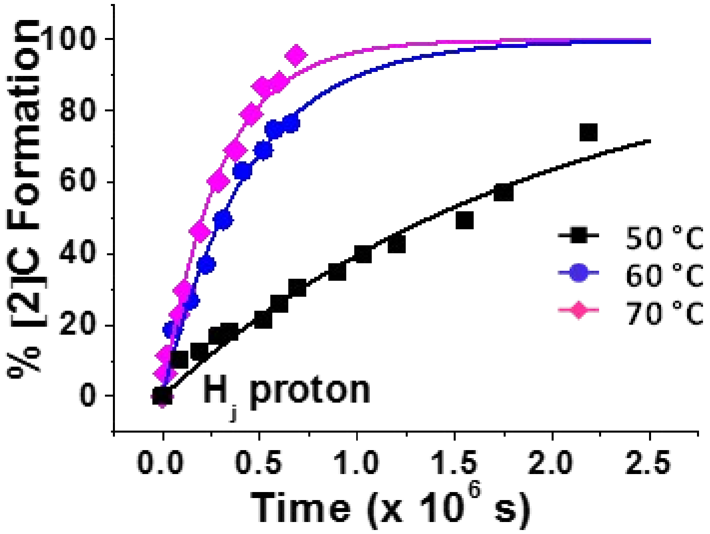

50 °C k_{obs} = 0.51(2) × 10^{-6} s^{-1}
60 °C k_{obs} = 2.30(8) × 10^{-6} s^{-1}
70 °C k_{obs} = 3.40(1) × 10^{-6} s^{-1}

Figure S2: Relative population of **Zn-[2]C** plotted against reaction time. Intensities of the H_j NMR proton signals of **Zn-TK** and **Zn-[2]C** were used to determine percent formation of **Zn-[2]C**. Three samples, each 0.85 mM solutions of **Zn-TK** in D_2O were heated to three different temperatures: 50, 60, or 70 °C. Solid lines in the plot represent the best fits for a first order kinetic process. k_{obs} values are presented in the box at the right. [2]C decomposed at the higher temperatures, which prevented the reaction from being monitored for as long as it was at 50 °C.

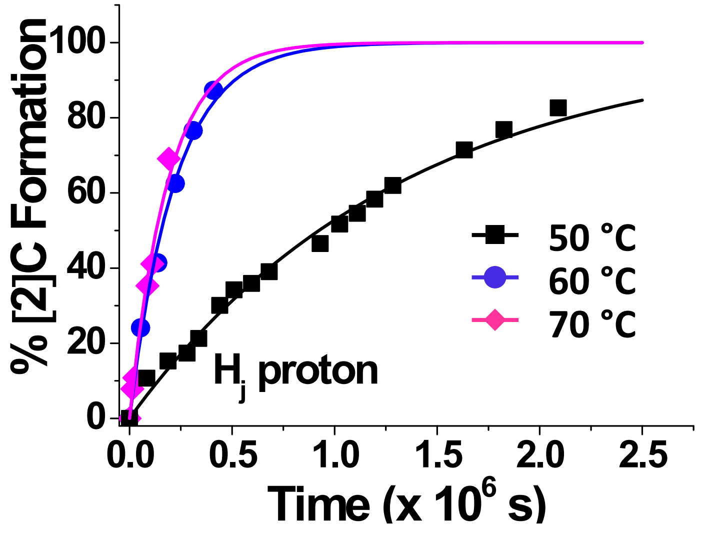

50 °C k_{obs} = 0.75(2) × 10^{-6} s^{-1}
60 °C k_{obs} = 4.50(2) × 10^{-6} s^{-1}
70 °C k_{obs} = 5.30(3) × 10^{-6} s^{-1}

Figure S3: Relative population of **Zn-[2]C** plotted against reaction time. Intensities of the H_j NMR proton signals of **Zn-TK** and **Zn-[2]C** were used to determine percent formation of **Zn-[2]C**. Three samples, each 3.4 mM solutions of **Zn-TK** in D_2O were heated to three different temperatures: 50, 60, or 70 °C. Solid lines in the plot represent the best fits for a first order kinetic process. k_{obs} values are presented in the box at the right. [2]C decomposed at the higher temperatures, which prevented the reaction from being monitored for as long as it was at 50 °C.

Monitoring of the H_h proton of Zn-[2]C

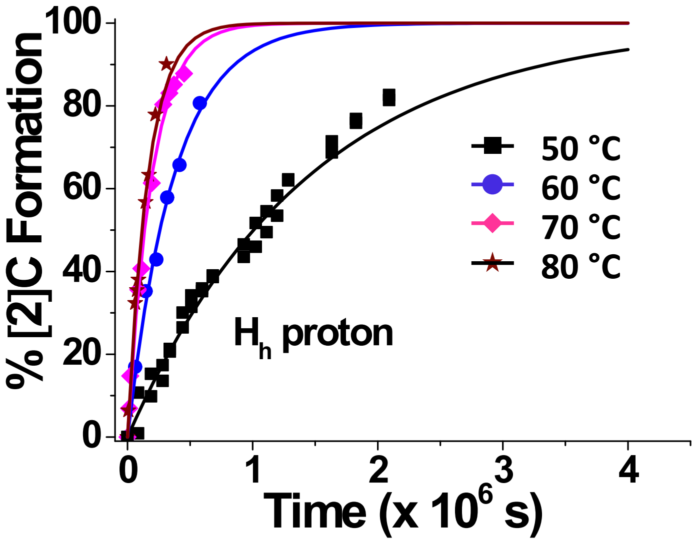

50 °C $k_{obs} = 0.69(2) \times 10^{-6}$ s^{-1}
60 °C $k_{obs} = 2.69(8) \times 10^{-6}$ s^{-1}
70 °C $k_{obs} = 5.10(2) \times 10^{-6}$ s^{-1}
80 °C $k_{obs} = 6.10(2) \times 10^{-6}$ s^{-1}

Figure S4: Relative population of **Zn-[2]C** plotted against reaction time. Intensities of the H_j NMR proton signals of **Zn-TK** and **Zn-[2]C** were used to determine percent formation of **Zn-[2]C**. Four samples, each 1.7 mM solutions of **Zn-TK** in D_2O were heated to four different temperatures: 50, 60, 70 or 80 °C. Solid lines in the plot represent the best fits for a first order kinetic process. k_{obs} values are presented in the box at the right. [2]C decomposed at the higher temperatures, which prevented the reaction from being monitored for as long as it was at 50 °C.

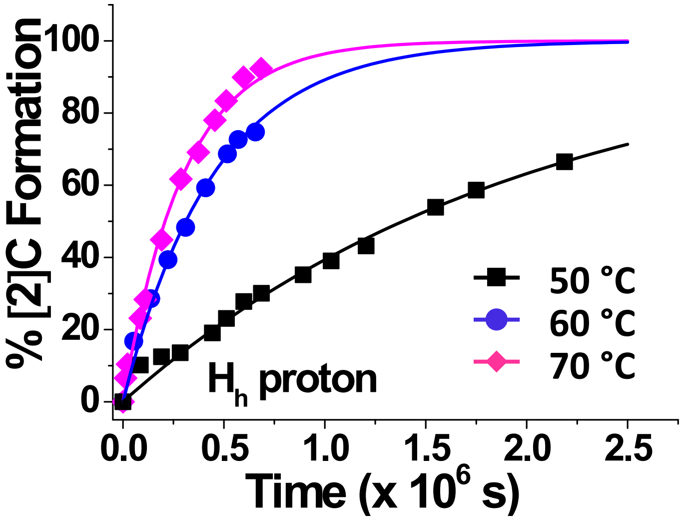

50 °C $k_{obs} = 0.50(2) \times 10^{-6}$ s^{-1}
60 °C $k_{obs} = 2.23(6) \times 10^{-6}$ s^{-1}
70 °C $k_{obs} = 3.33(9) \times 10^{-6}$ s^{-1}

Figure S5: Relative population of **Zn-[2]C** plotted against reaction time. Intensities of the H_j NMR proton signals of **Zn-TK** and **Zn-[2]C** were used to determine percent formation of **Zn-[2]C**. Three samples, each 0.85 mM solutions of **Zn-TK** in D_2O were heated to three different temperatures: 50, 60, or 70 °C. Solid lines in the plot represent the best fits for a first order kinetic process. k_{obs} values are presented in the box at the right. [2]C decomposed at the higher temperatures, which prevented the reaction from being monitored for as long as it was at 50 °C.

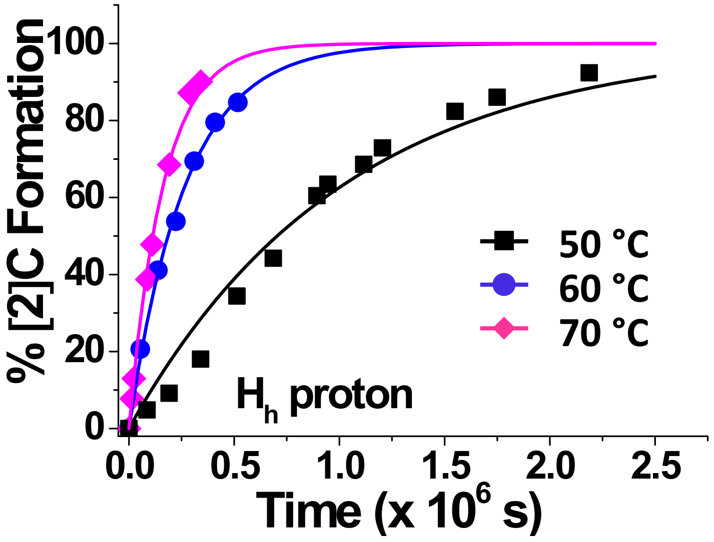

50 °C k_{obs} = 0.98(5) × 10^{-6} s^{-1}
60 °C k_{obs} = 3.74(9) × 10^{-6} s^{-1}
70 °C k_{obs} = 6.10(2) × 10^{-6} s^{-1}

Figure S6: Relative population of **Zn-[2]C** plotted against reaction time. Intensities of the H_j NMR proton signals of **Zn-TK** and **Zn-[2]C** were used to determine percent formation of **Zn-[2]C**. Three samples, each 3.4 mM solutions of **Zn-TK** in D_2O, were heated to three different temperatures: 50, 60, or 70 °C. Solid lines in the plot represent the best fits for a first order kinetic process. k_{obs} values are presented in the box at the right. [2]C decomposed at the higher temperatures, which prevented the reaction from being monitored for as long as it was at 50 °C.

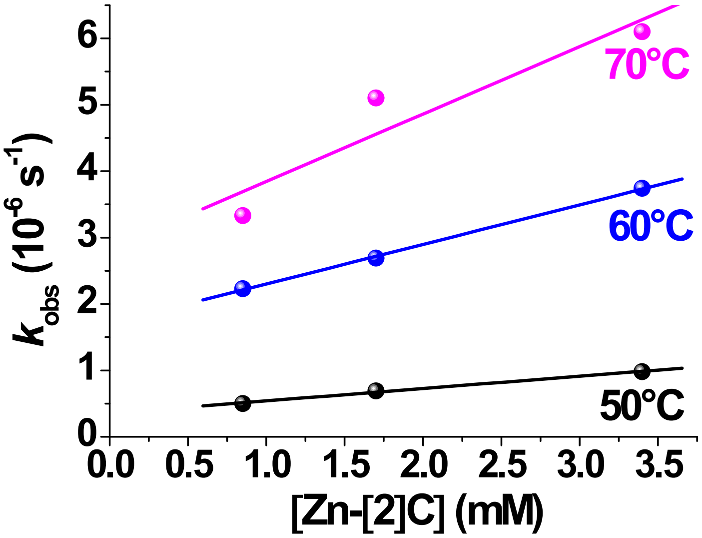

Figure S7: Variation of the k_{obs} (s^{-1}) as a function of **Zn-2[C]** concentration which shows that the interconversion is complex and cannot be considered to have a simple rate-limiting step. Solvent: D_2O.

Calculation of the apparent energy of activation of Zn-[2]C formation using an Arrhenius plot

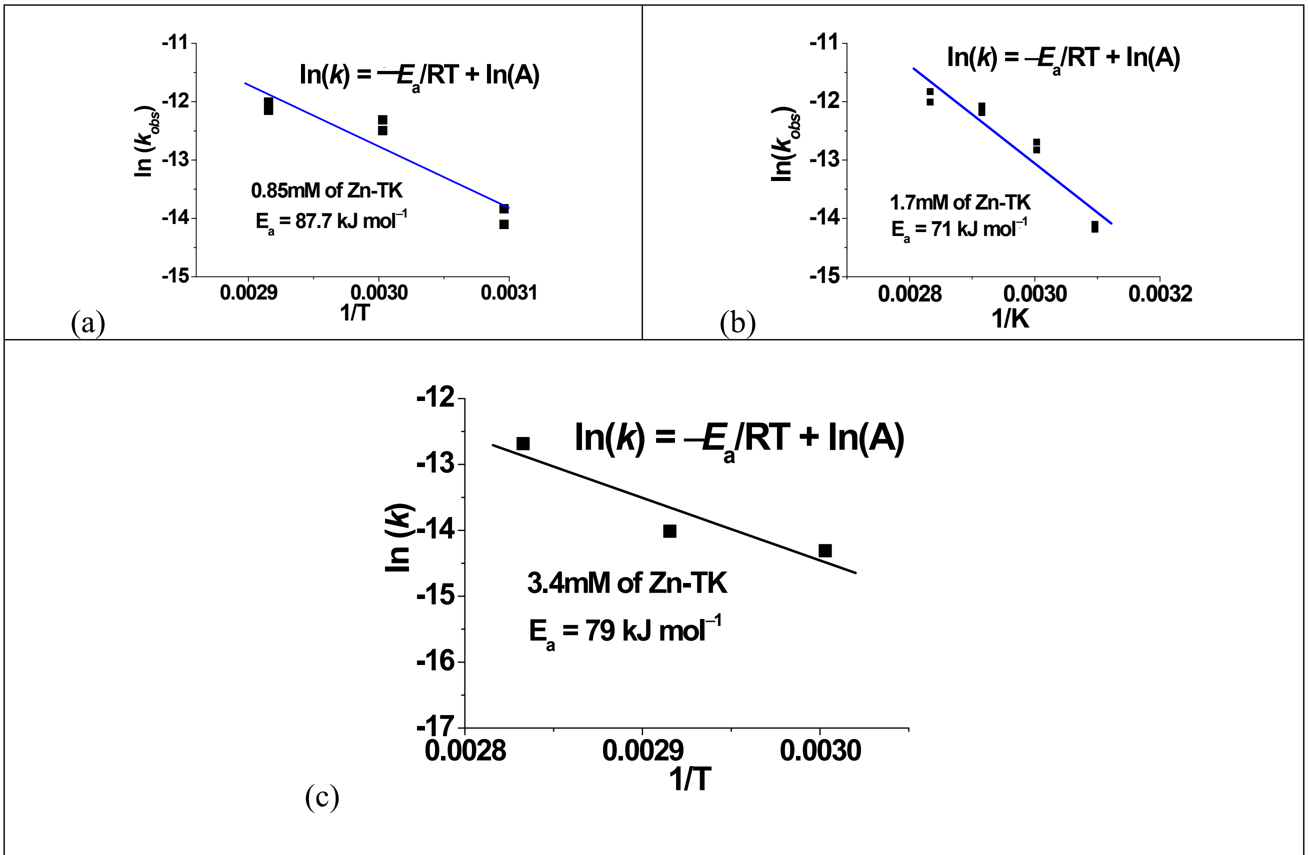

(a)

(b)

(c)

Figure S8: Calculation of the apparent activation energy for the formation of **Zn-[2]C** using three different initial concentrations of **Zn-TK**: **(a)** 0.85 mM, **(b)** 1.7 mM and **(c)** 3.4 mM. using H_j and H_h protons of **Zn-[2]C**.

Calculation of the apparent ΔH^0 and ΔS^0 using van't hoff equation

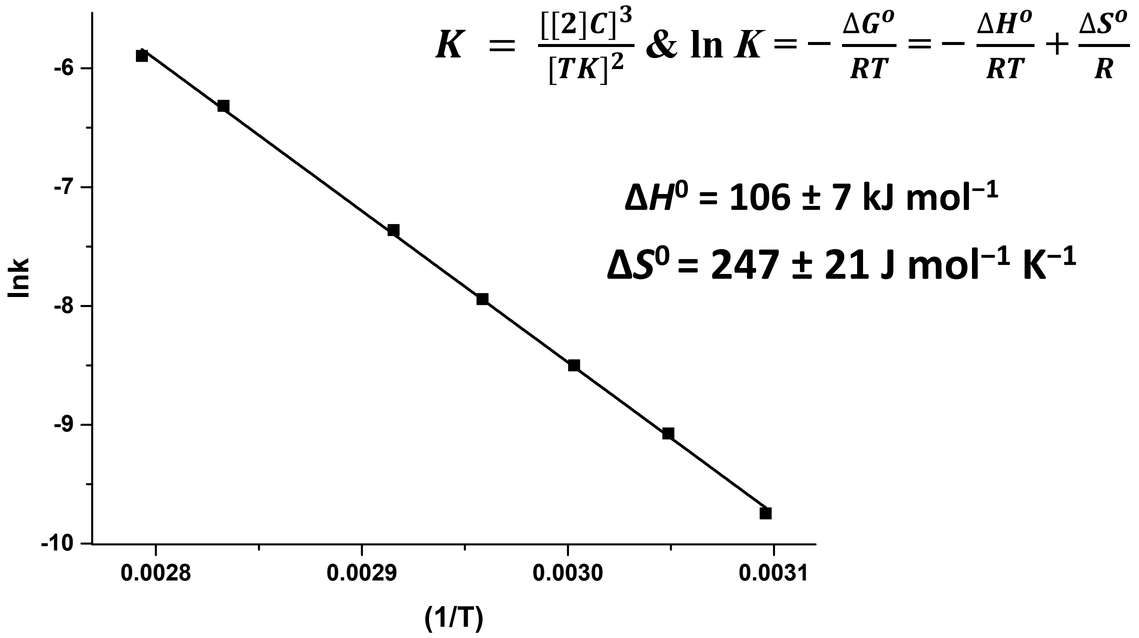
$$K = \frac{[[2]C]^3}{[TK]^2} \;\&\; \ln K = -\frac{\Delta G^o}{RT} = -\frac{\Delta H^o}{RT} + \frac{\Delta S^o}{R}$$

$\Delta H^0 = 106 \pm 7$ kJ mol^{-1}

$\Delta S^0 = 247 \pm 21$ J mol^{-1} K^{-1}

Figure S8a: Calculation of the apparent ΔH^0 and ΔS^0 using 1.7 mM initial concentrations of Zn-TK .

High resolution mass spectrometric kinetic analysis of the transformation of Zn-TK into Zn-[2]C

HRMS analysis reveals the presence of a pool of intermediates at every stage of the reaction.

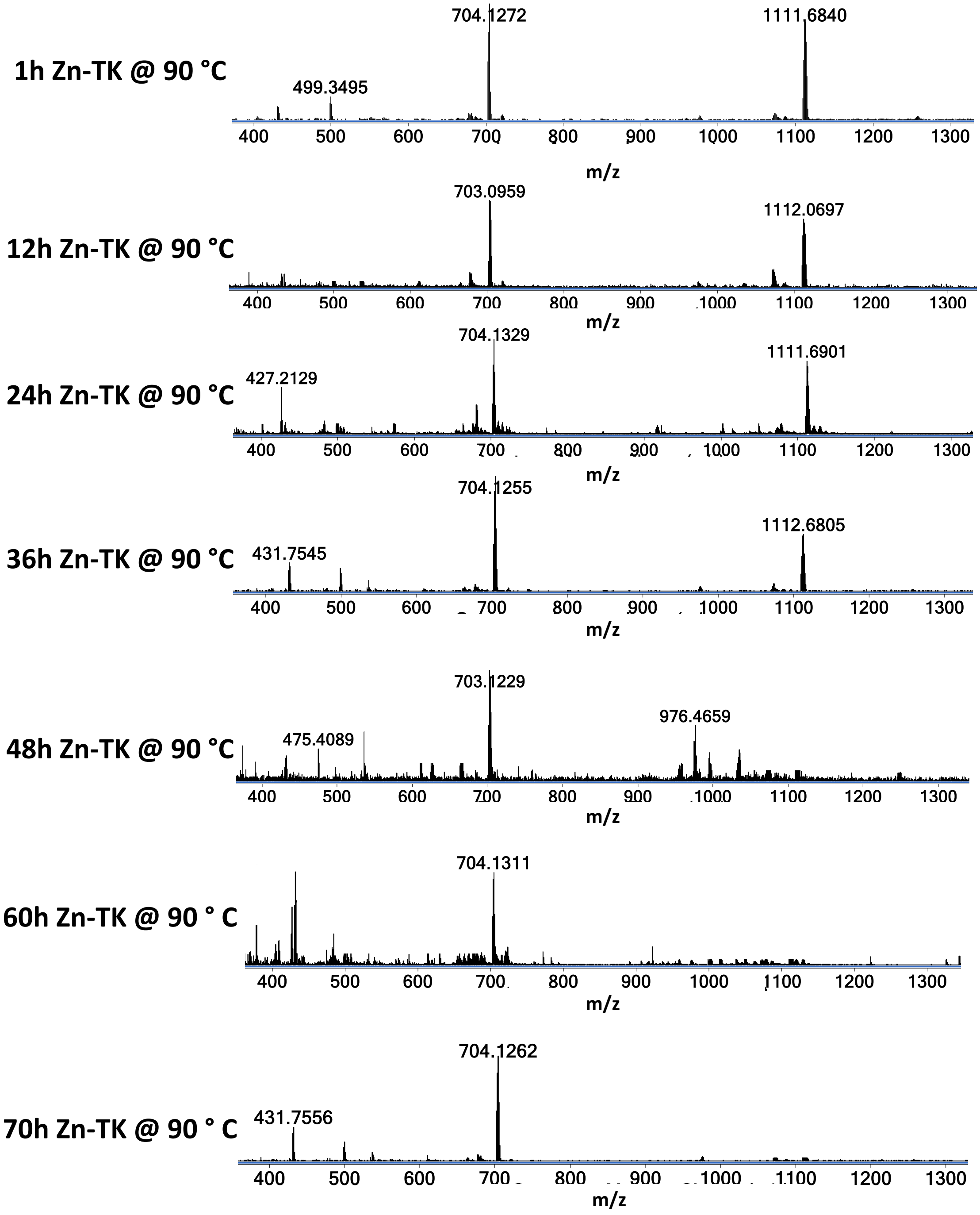

Figure S9: High resolution mass spectrograms of a **Zn-TK** solution heated at 90 °C and sampled over time. The evolution of the spectra reflects the progress of the transformation of **Zn-TK** into **Zn-[2]C**.

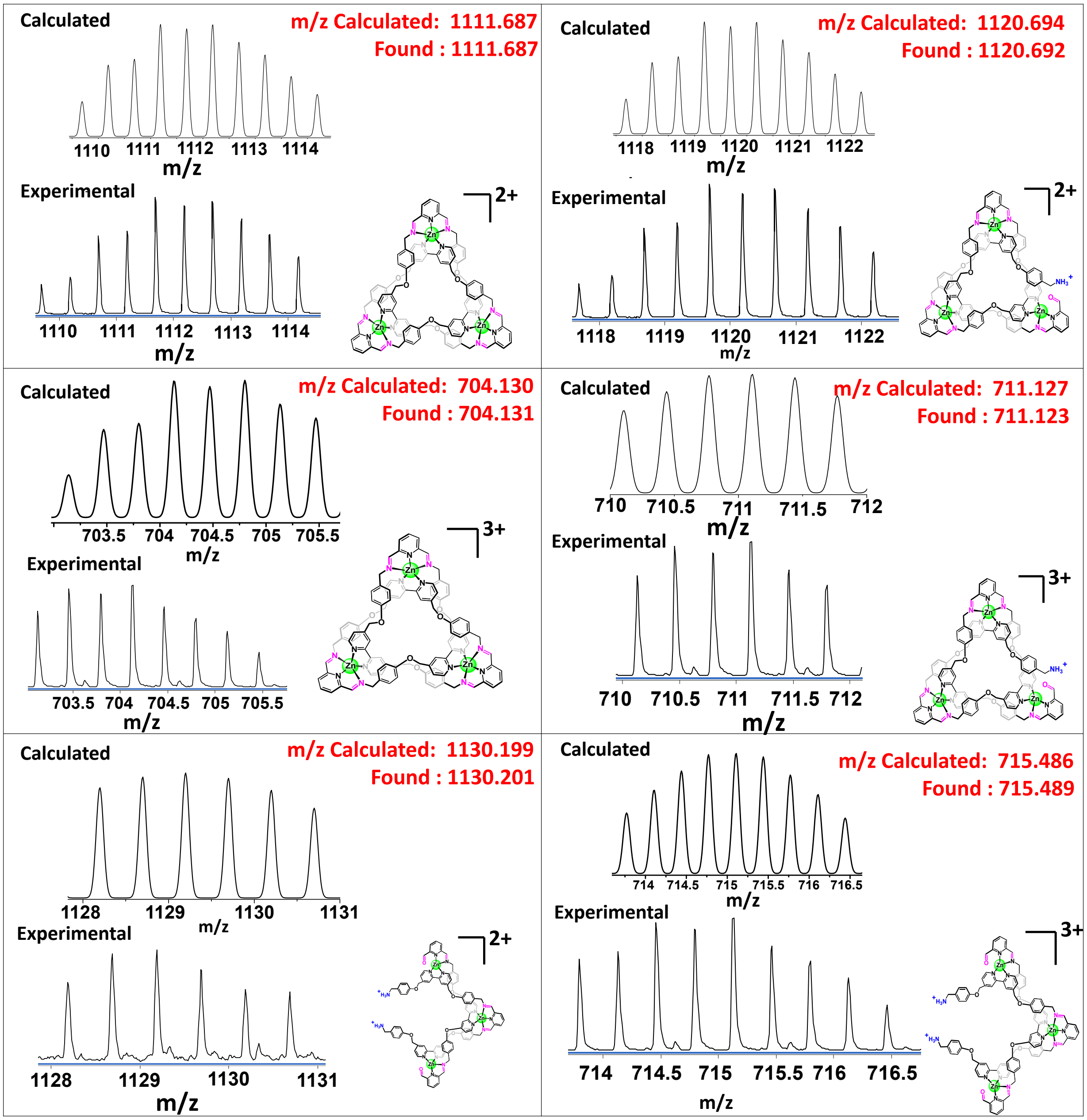
Calculated
m/z Calculated: 1111.687
Found : 1111.687
1110 1111 1112 1113 1114
m/z
Experimental
1110 1111 1112 1113 1114
m/z
2+
Calculated
m/z Calculated: 1120.694
Found : 1120.692
1118 1119 1120 1121 1122
m/z
Experimental
1118 1119 1120 1121 1122
m/z
2+
Calculated
m/z Calculated: 704.130
Found : 704.131
703.5 704 704.5 705 705.5
m/z
Experimental
703.5 704 704.5 705 705.5
m/z
3+
Calculated
m/z Calculated: 711.127
Found : 711.123
710 710.5 711 711.5 712
m/z
Experimental
710 710.5 711 711.5 712
m/z
3+
Calculated
m/z Calculated: 1130.199
Found : 1130.201
1128 1129 1130 1131
m/z
Experimental
1128 1129 1130 1131
m/z
2+
Calculated
m/z Calculated: 715.486
Found : 715.489
714 714.5 715 715.5 716 716.5
m/z
Experimental
714 714.5 715 715.5 716 716.5
m/z
3+
Zn
N
O

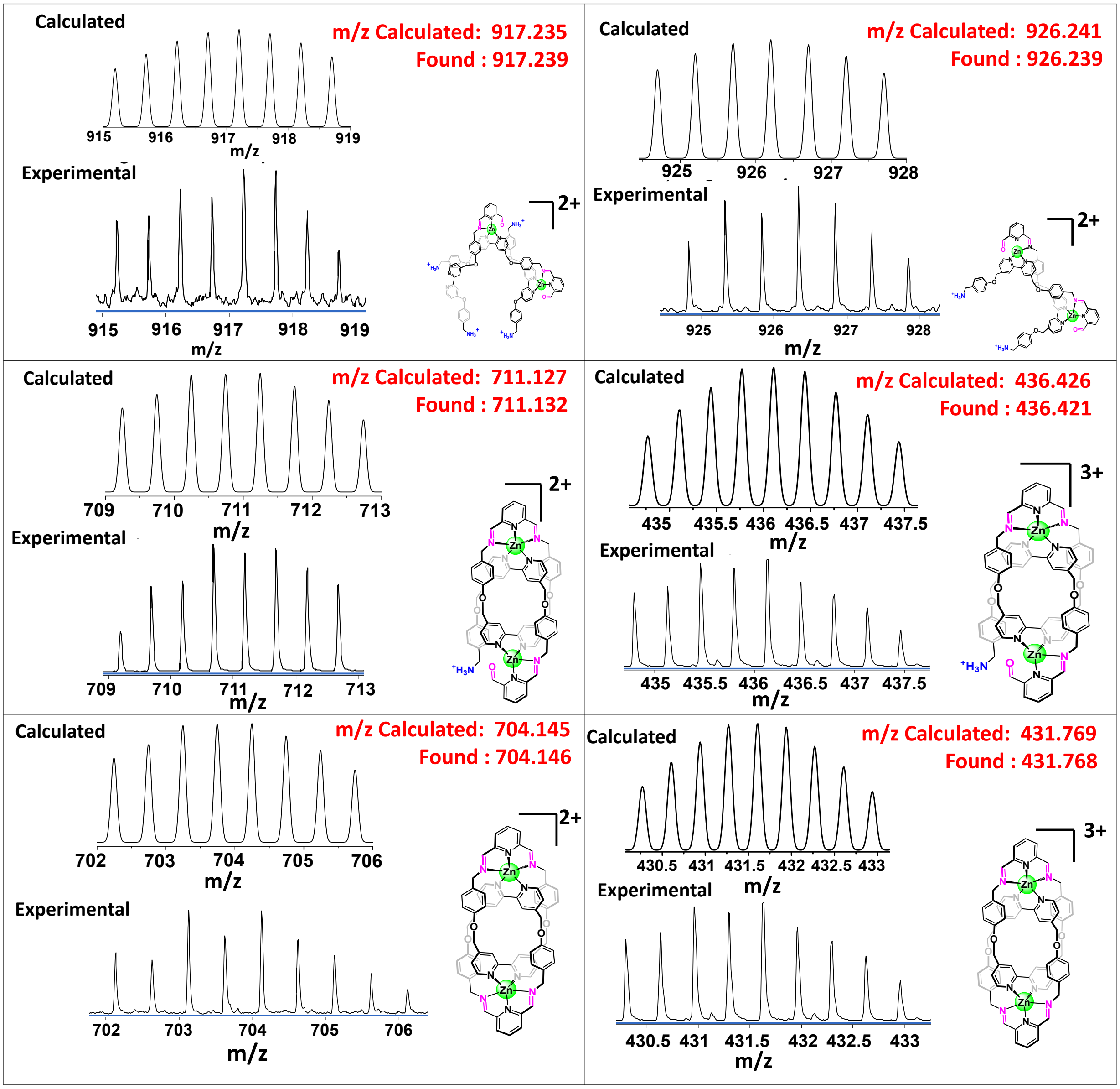
Calculated
m/z Calculated: 917.235
Found : 917.239
915 916 917 918 919
m/z
Experimental
915 916 917 918 919
m/z
2+
Zn
Zn
Calculated
m/z Calculated: 926.241
Found : 926.239
925 926 927 928
Experimental
925 926 927 928
m/z
2+
Zn
Zn
Calculated
m/z Calculated: 711.127
Found : 711.132
709 710 711 712 713
m/z
Experimental
709 710 711 712 713
m/z
2+
Zn
Zn
N
O
^+H_3N
Calculated
m/z Calculated: 436.426
Found : 436.421
435 435.5 436 436.5 437 437.5
m/z
Experimental
435 435.5 436 436.5 437 437.5
m/z
3+
Zn
Zn
N
O
^+H_3N
Calculated
m/z Calculated: 704.145
Found : 704.146
702 703 704 705 706
m/z
Experimental
702 703 704 705 706
m/z
2+
Zn
Zn
N
O
Calculated
m/z Calculated: 431.769
Found : 431.768
430.5 431 431.5 432 432.5 433
Experimental
m/z
430.5 431 431.5 432 432.5 433
m/z
3+
Zn
Zn
N
O

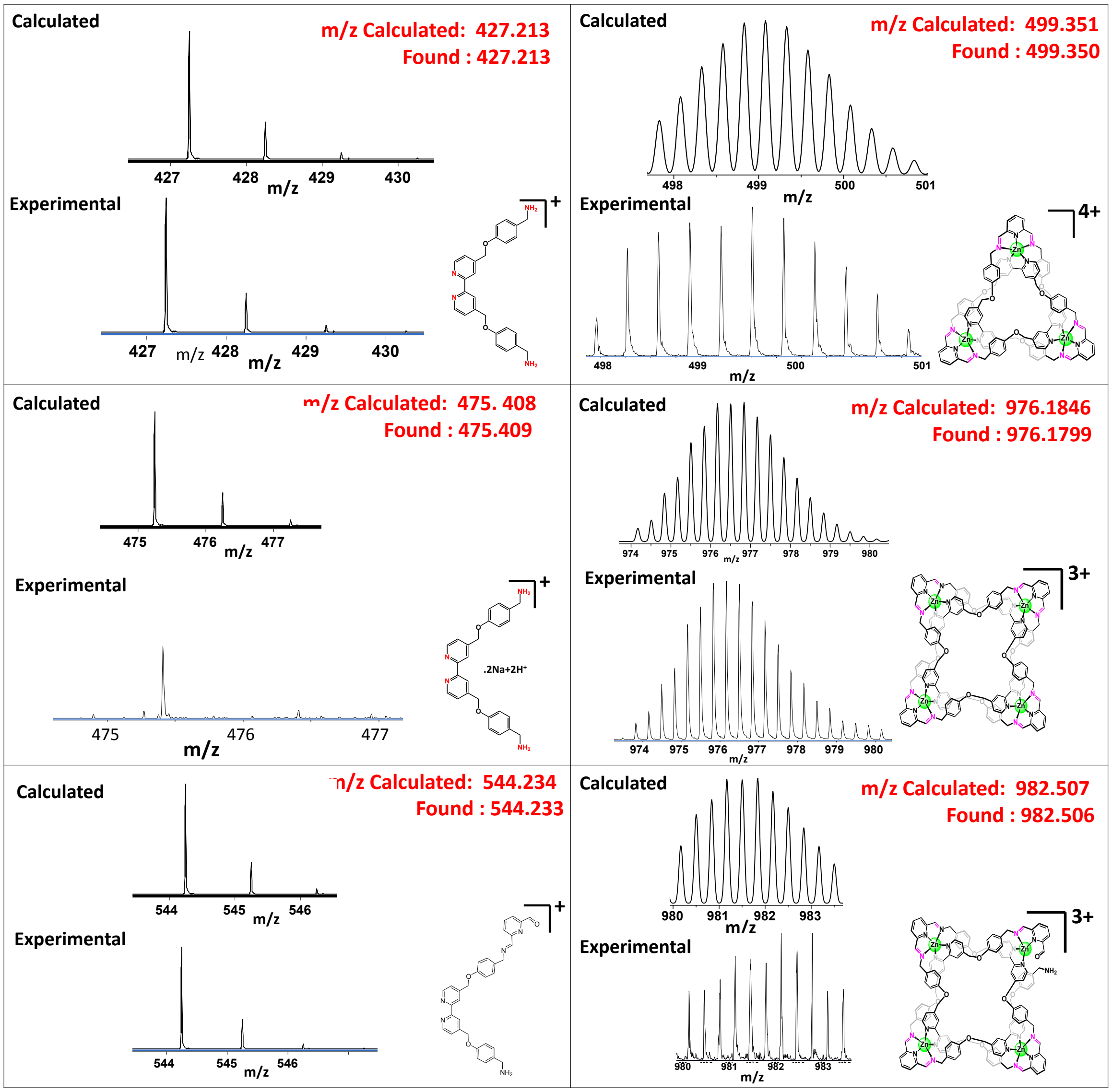

Figure S10: Expansions of the isotopic distribution patterns of the intermediates (represented in the upper right of each box) identified by HRMS during the thermal transformation of **Zn-TK** into **Zn-[2]C**.

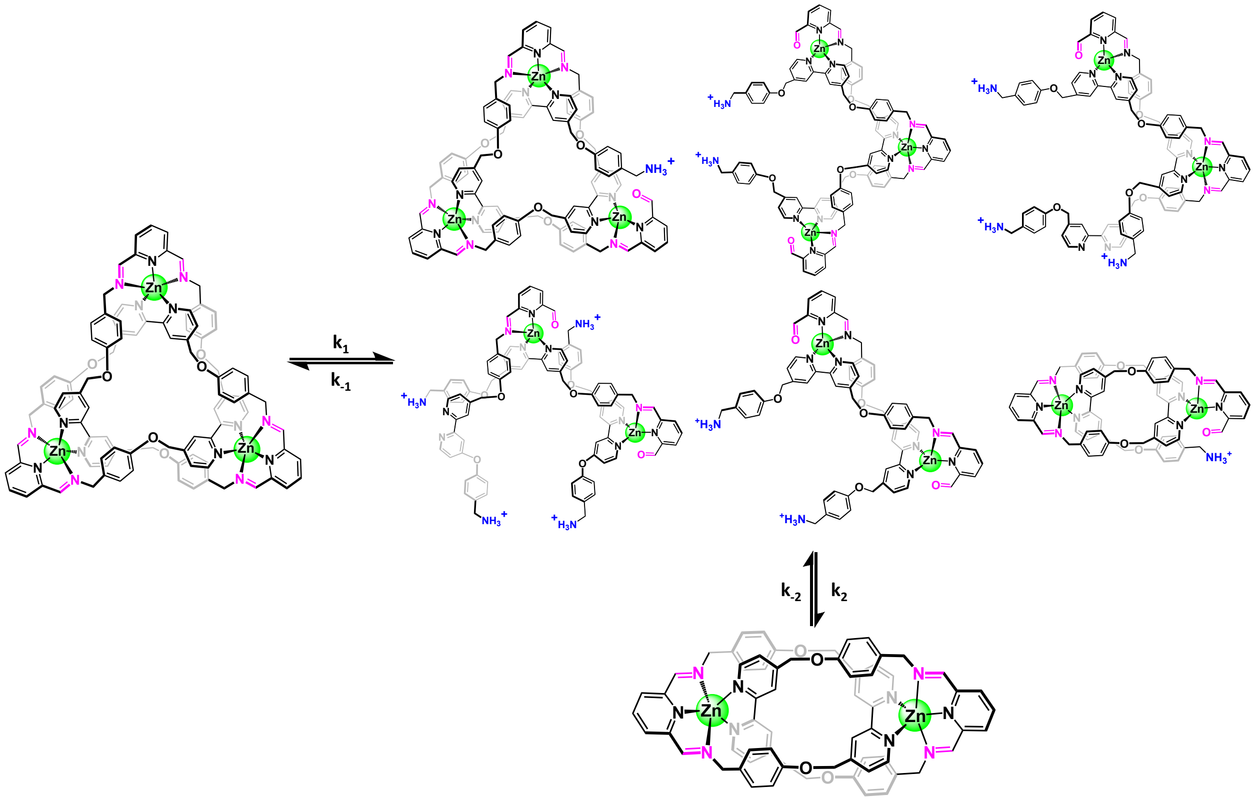

Figure S11a: Intermediate species identified by HRMS during the thermal conversion of **Zn-TK** into **Zn-[2]C**. This study revealed the complexity of the mechanism of transformation.

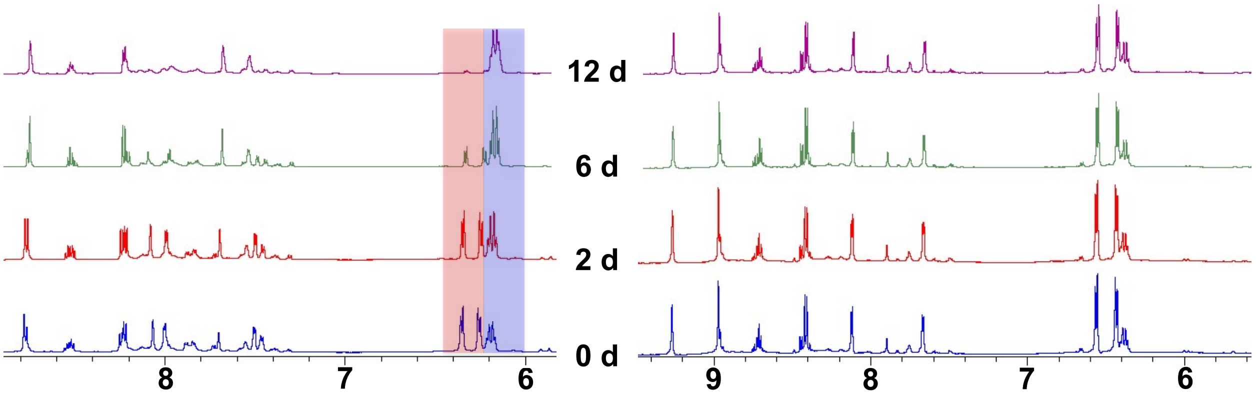

Figure S11b: (Left) Downfield regions of the ^{1}H NMR spectra measured during the interconversion of **Zn-TK** into **Zn-[2]C** in the absence of bromide. (Right) Downfield regions of the ^{1}H NMR spectra measured during the interconversion of **Zn-TK** into **Zn-[2]C** in the presence of two equivalents of tetrabutylammonium bromide. Solvent: D$_2$O, T = 323 K.

3. Transformation of Cd-TK into Cd-[2]C

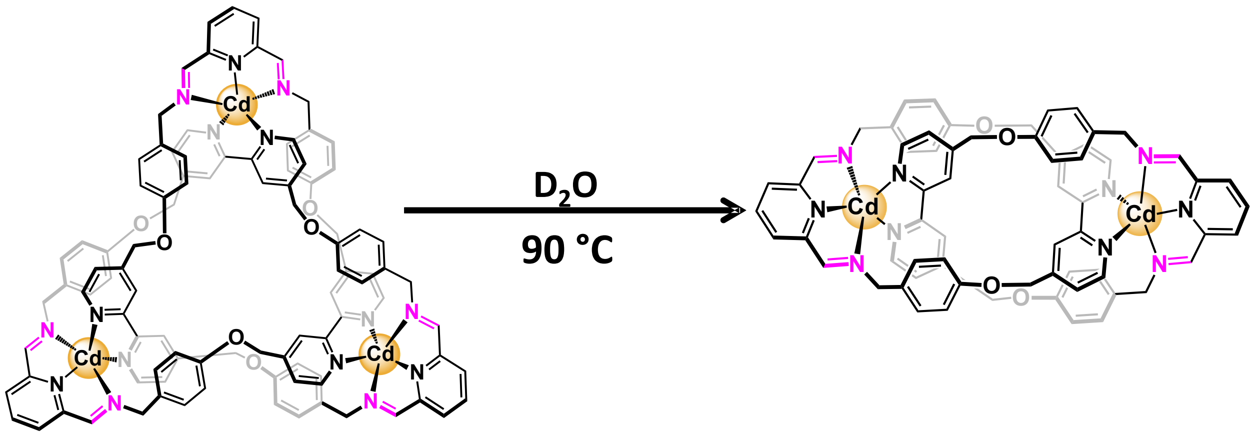

A 1.7 mM solution of **Cd-TK** in D$_2$0 was placed in an NMR tube and heated to 90 ºC in an oil bath. The progress of the reaction was monitored by ^{1}H NMR spectroscopy at room temperature and regular time intervals. After reaction completion, **Zn-[2]C** was precipitated upon addition of a mixed solvent of isopropanol and THF (2:1). The precipitate was washed four times with the hot solvent mixture to remove side-products, including open chain cadmium complexes which were estimated to amount to less than 10 mol % of the total product mixture. The final precipitate was dried under vacuum for 4 h and characterized by ^{1}H and ^{13}C NMR spectroscopy and HRMS.

Cd-[2]C: 85 %; ^{1}H NMR (500 MHz, D$_2$O, 25 °C): δ 4.74 (s, 8H, Ar-C*H$_2$*), 5.04 (s, 8H, Ar-C*H$_2$*), 6.09 (d, 8H, *J* = 7.6 Hz, Ar-*H*),), 6.49 (d, 8H, *J* = 7.8 Hz, Ar-*H*), 7.61 (d, 4H, *J* = 5.2 Hz, Ar-*H*), 8.08 (d, 4H, *J* = 5.1 Hz, Ar-*H*), 8.22 (m, 8H, Ar-*H*), 8.51 (t, 2H, *J* = 7.7 Hz, Ar-*H*), 8.89 (s, 4H, Ar-*H*); ^{13}C NMR (125 MHz, MeOH-d4, 25 °C): δ 62.6, 66.4, 114.0, 118.6 (q, $^{2}J_{C\text{-}F}$ = 263 Hz, TFA), 120.6, 124.7, 128.9, 129.3, 129.9, 137.8, 143.2, 148.1, 148.5, 150.4, 156.7, 158.5, 161.2 (q, $^{3}J_{C\text{-}F}$ = 33 Hz. TFA); MS (ESI-MS): m/z Calcd for $(C_{70}H_{54}Cd_2F_6N_{10}O_8)^{2+}$: 751.104 [M–2TFA]$^{2+}$, found: 751.105 [M–2TFA]$^{2+}$.

The transformation of **Cd-TK** into **Cd-[2]C** was monitored in solution by ^{1}H NMR spectroscopy at regular time intervals.

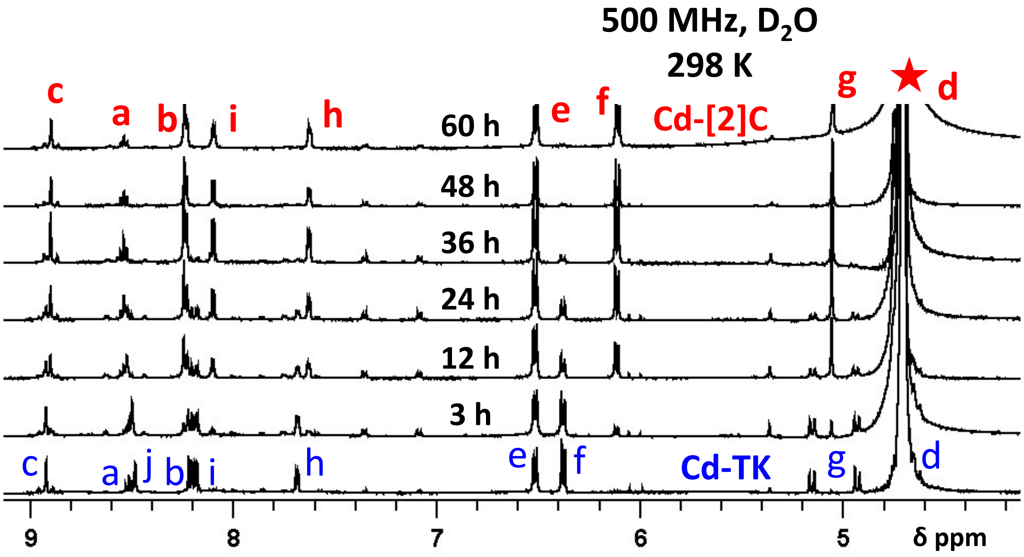

Figure S12: Stacked ^{1}H NMR spectra of a 1.7mM solution of **Cd-TK** in D_2O acquired at 500 MHz, 298 K and at regular time intervals. The evolution of the spectra reflects the progress of the transformation of **Cd-TK** into **Cd-[2]C**.

The transformation of **Cd-TK** into **Cd-[2]C** was also monitored by HRMS in the gas phase at regular time intervals.

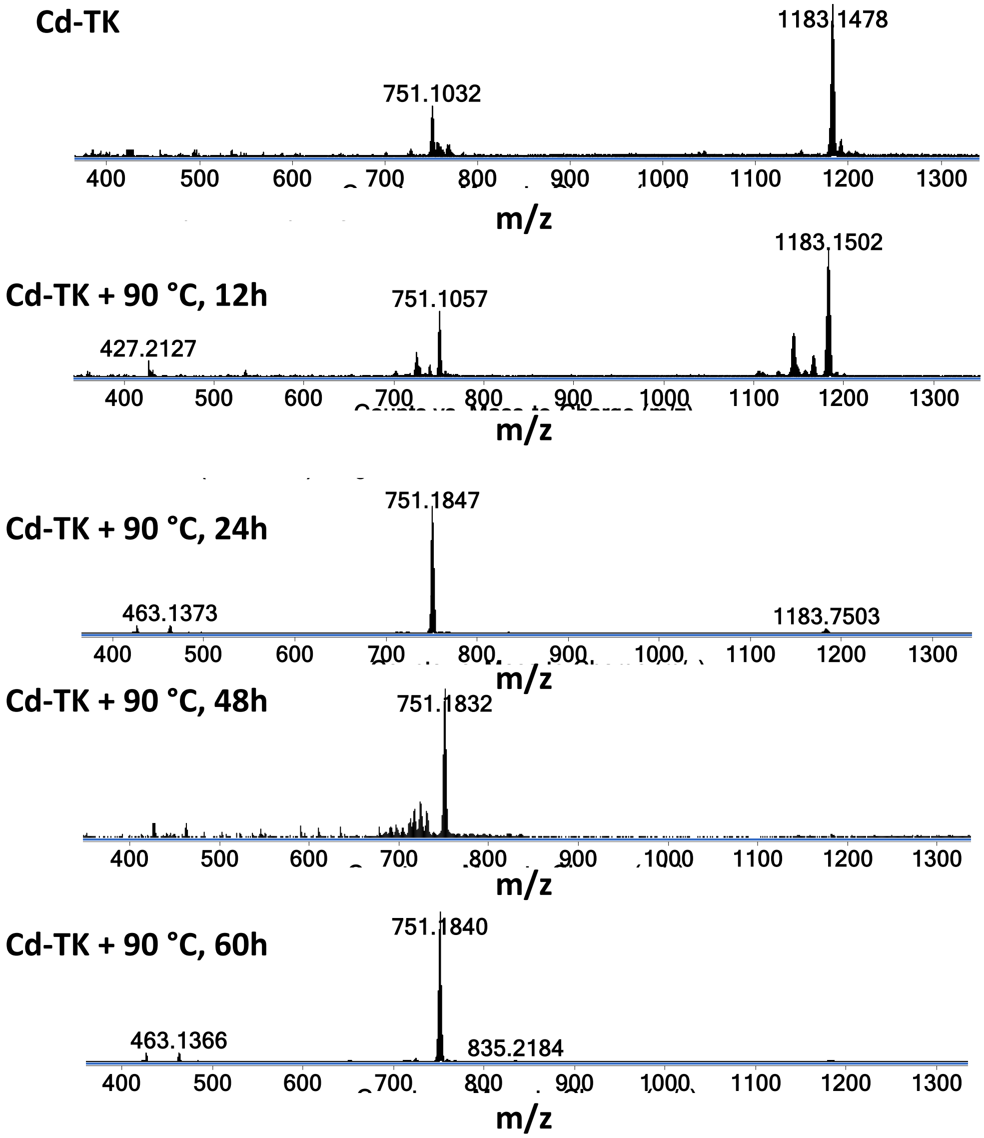

Figure S13: High resolution mass spectrograms of a **Cd-TK** solution heated @ 90 °C and sampled over time. The evolution of the spectrograms reflects the progress of the transformation of **Cd-TK** into **Cd-[2]C**.

4.0. Transformation of Cd-TK into Zn-[2]C

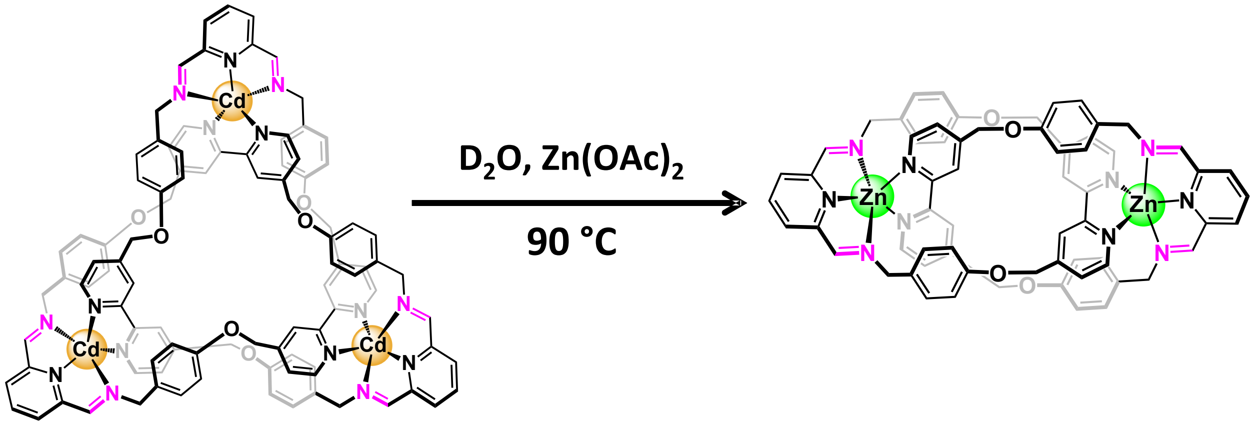

Cd-TK (2.8 mg; 0.023 mM) was added to zinc acetate (10.1 mg, 20 equivalents) in a 1:1 mixture of 0.6 mL of CD_3OD and D_2O. The samples were prepared in NMR tubes subjected to 90 °C in oil bath and the progress of the reactions was monitored by ^{1}H NMR spectroscopy at various time intervals. After reaction completion, **Zn-[2]C** was precipitated upon addition of a mixed solvent of isopropanol and THF (2:1). The precipitate was washed four times with the hot solvent mixture to remove excess zinc acetate and side-products, including open chain complexes which were estimated to amount to less than 10 mol % of the total product mixture. The final precipitate was dried under vacuum for 4 h and characterized by ^{1}H and ^{13}C NMR spectroscopy and HRMS.

Zn-[2]C: Yield: 86 %. ^{1}H NMR (500MHz, D_2O, 25 °C): δ 5.03 (s, 8H, Ar-C*H₂*), 5.43 (s, 8H, Ar-C*H₂*), 6.60 (ABq, 16H, *J* = 12 Hz, Ar-*H*), 7.97 (d, 4H, *J* = 4.5 Hz, Ar-*H*), 8.10 (s, 4H, Ar-*H*), 8.37 (s, br, 4H, Ar-*H*), 8.64 (d, 4H, *J* = 8.2 Hz, Ar-*H*), 8.94 (t, 2H, *J* = 7.8 Hz, Ar-*H*), 9.16 (s, 4H, Ar-*H*); ^{13}C NMR (75 MHz, MeOD-d_4, 25 °C): δ 63.6, 68.3, 116.6, 117.7 (q, $^2J_{C\text{-}F}$ = 255 Hz, TFA), 122.1, 127.0, 128.0, 129.7, 130.1, 131.0, 135.4, 148.4, 148.8, 148.9, 152.9, 158.4, 161.7 (q, $^3J_{C\text{-}F}$ = 34.5 Hz. TFA); MS (ESI-HRMS): m/z Calcd for $(C_{70}H_{58}F_6N_{10}O_8Zn_2)^{2+}$: 704.146 $[M{-}2TFA]^{2+}$, found: 704.147 [M−2TFA]$^{2+}$, m/z Calcd for $(C_{68}H_{58}F_3N_{10}O_6Zn_2)^{3+}$: 431.769 [M−3TFA]$^{3+}$, found: 431.768 [M−3TFA]$^{3+}$.

To track the reaction carefully, the transformation of **Cd-TK** into **Zn-[2]C** was monitored using ^{1}H NMR in solution and HR mass spectrometry at regular time intervals.

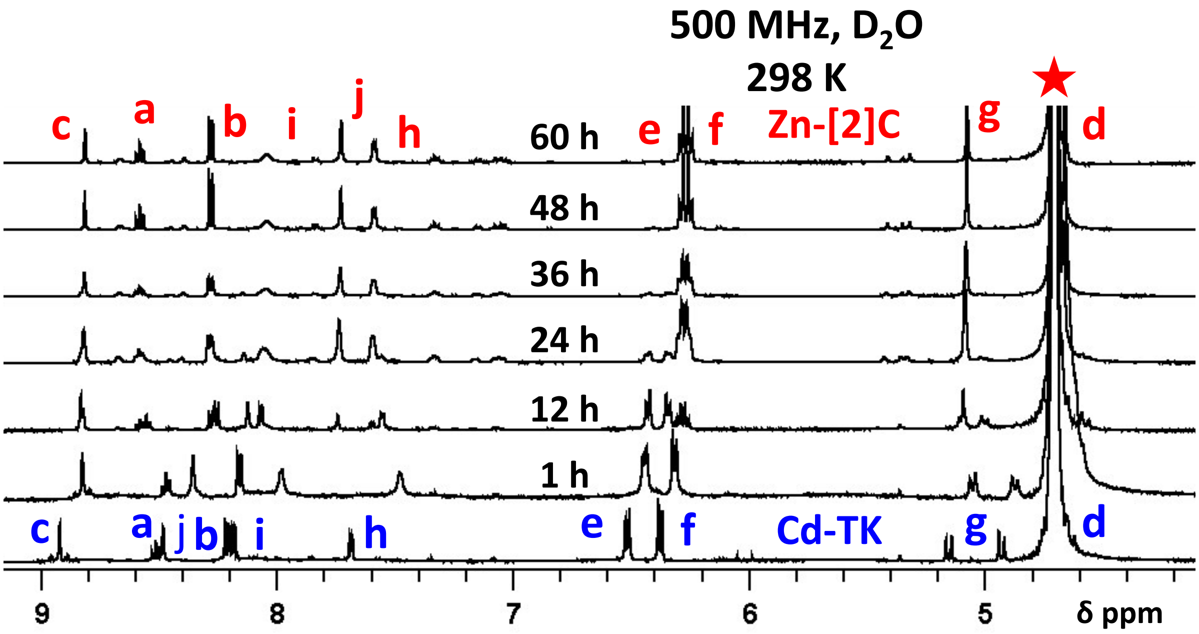

Figure S14: Stacked ^{1}H NMR spectra of a 1.7 mM solution of **Cd-TK** in D_2O with excess $Zn(OAc)_2$ acquired at 500 MHz, 25 °C and at regular time intervals. The evolution of the spectra reflects the progress of the transformation of **Cd-TK** into **Zn-[2]C**.

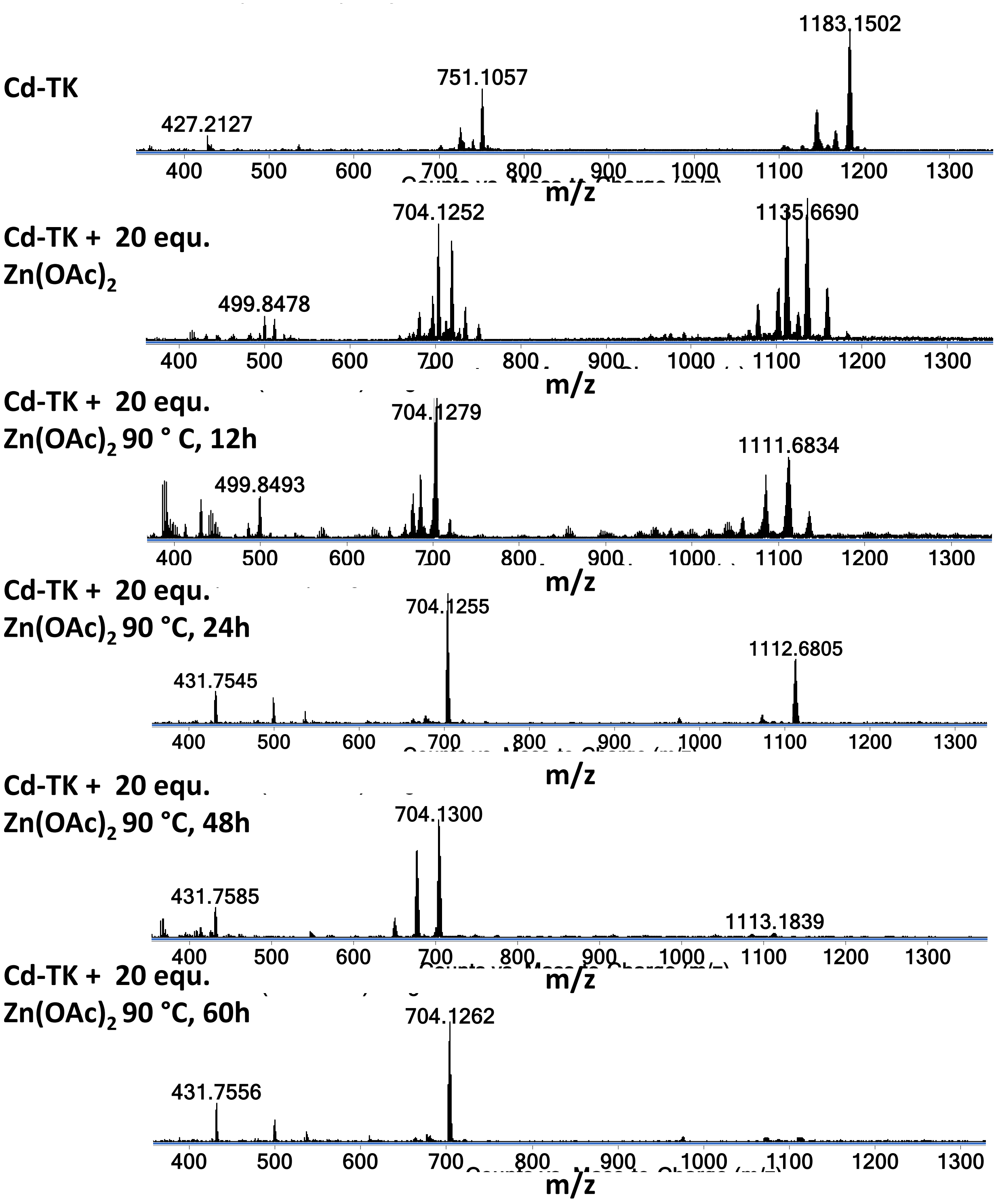

Figure S15a: High resolution mass spectrograms of a **Cd-TK** solution heated at 90 °C and sampled over time. The evolution of the spectrograms reflects the progress of the transformation of **Cd-TK** into **Zn-[2]C**.

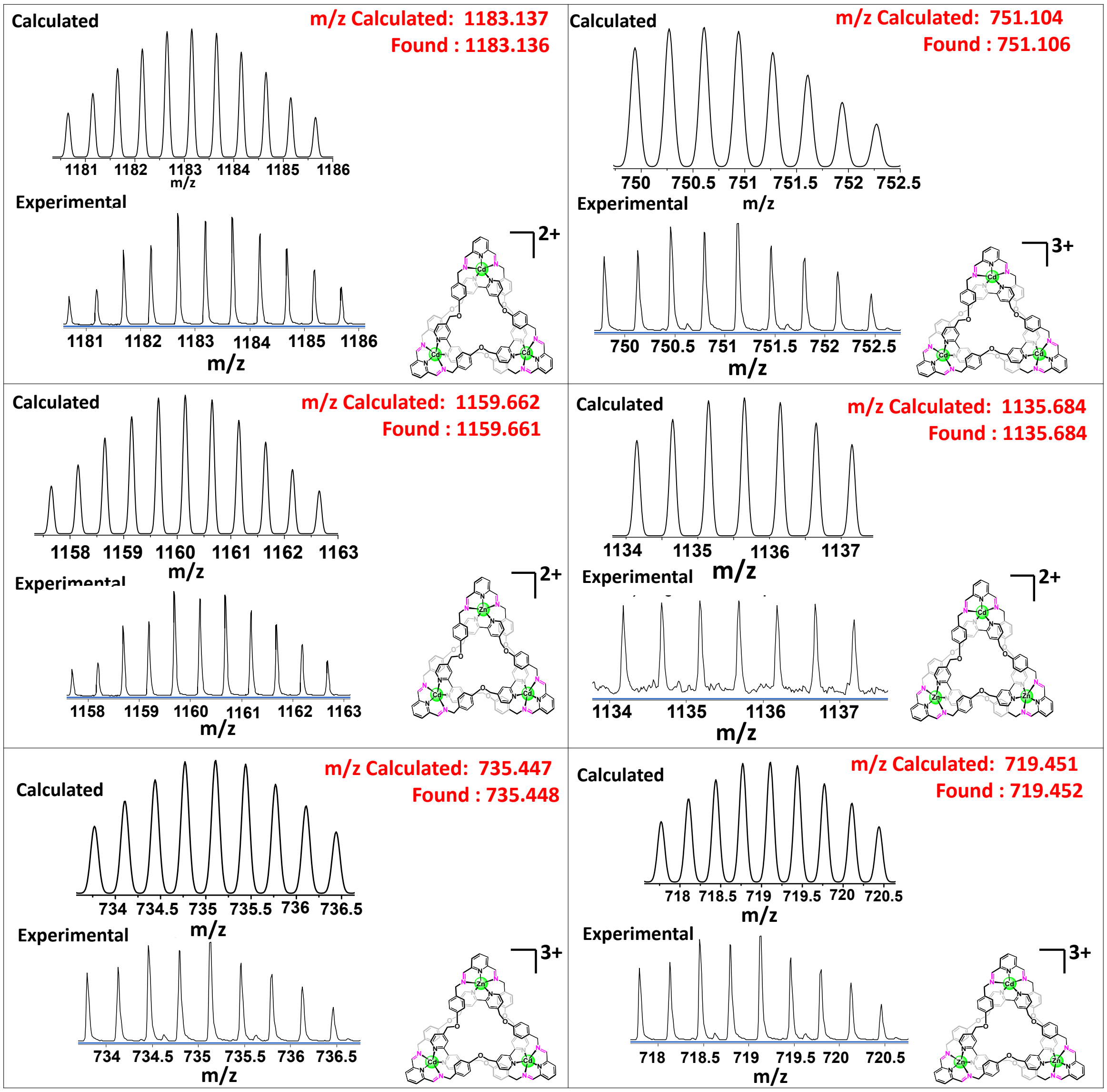

Calculated
m/z Calculated: 1183.137
Found : 1183.136
1181 1182 1183 1184 1185 1186
m/z
Experimental
1181 1182 1183 1184 1185 1186
m/z
2+
Cd
Cd
Cd
Calculated
m/z Calculated: 751.104
Found : 751.106
750 750.5 751 751.5 752 752.5
m/z
Experimental
750 750.5 751 751.5 752 752.5
m/z
3+
Cd
Cd
Cd
Calculated
m/z Calculated: 1159.662
Found : 1159.661
1158 1159 1160 1161 1162 1163
m/z
Experimental
1158 1159 1160 1161 1162 1163
m/z
2+
Zn
Cd
Cd
Calculated
m/z Calculated: 1135.684
Found : 1135.684
1134 1135 1136 1137
m/z
Experimental
1134 1135 1136 1137
m/z
2+
Cd
Zn
Zn
Calculated
m/z Calculated: 735.447
Found : 735.448
734 734.5 735 735.5 736 736.5
m/z
Experimental
734 734.5 735 735.5 736 736.5
m/z
3+
Zn
Cd
Cd
Calculated
m/z Calculated: 719.451
Found : 719.452
718 718.5 719 719.5 720 720.5
m/z
Experimental
718 718.5 719 719.5 720 720.5
m/z
3+
Cd
Zn
Zn

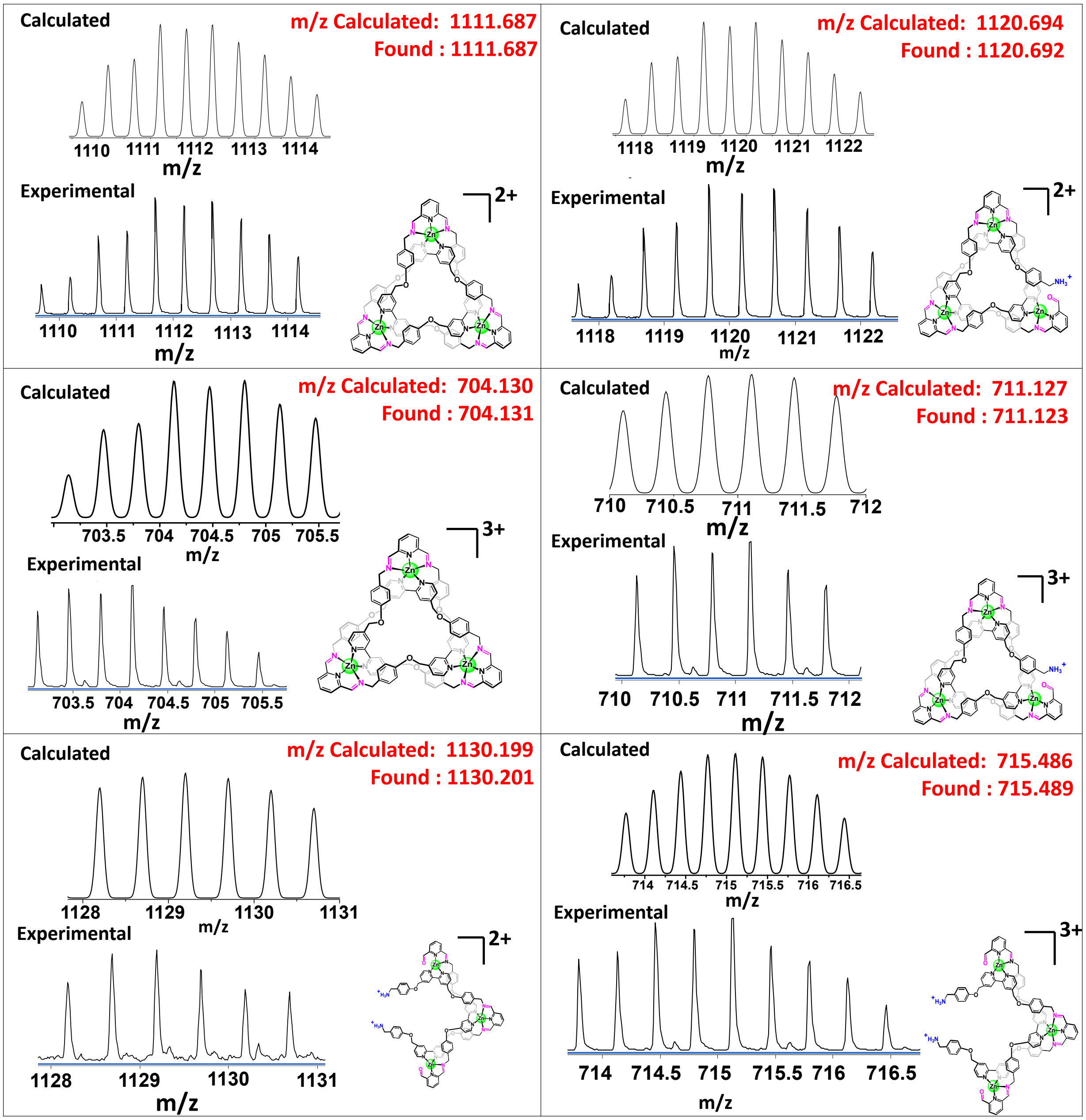
Calculated
m/z Calculated: 1111.687
Found : 1111.687
1110 1111 1112 1113 1114
m/z
Experimental
1110 1111 1112 1113 1114
m/z
2+
Zn
Calculated
m/z Calculated: 1120.694
Found : 1120.692
1118 1119 1120 1121 1122
m/z
Experimental
1118 1119 1120 1121 1122
m/z
2+
Zn
NH3+
Calculated
m/z Calculated: 704.130
Found : 704.131
703.5 704 704.5 705 705.5
m/z
Experimental
703.5 704 704.5 705 705.5
m/z
3+
Calculated
m/z Calculated: 711.127
Found : 711.123
710 710.5 711 711.5 712
m/z
Experimental
710 710.5 711 711.5 712
m/z
3+
Calculated
m/z Calculated: 1130.199
Found : 1130.201
1128 1129 1130 1131
m/z
Experimental
1128 1129 1130 1131
m/z
2+
+H3N
Calculated
m/z Calculated: 715.486
Found : 715.489
714 714.5 715 715.5 716 716.5
m/z
Experimental
714 714.5 715 715.5 716 716.5
m/z
3+
+H3N

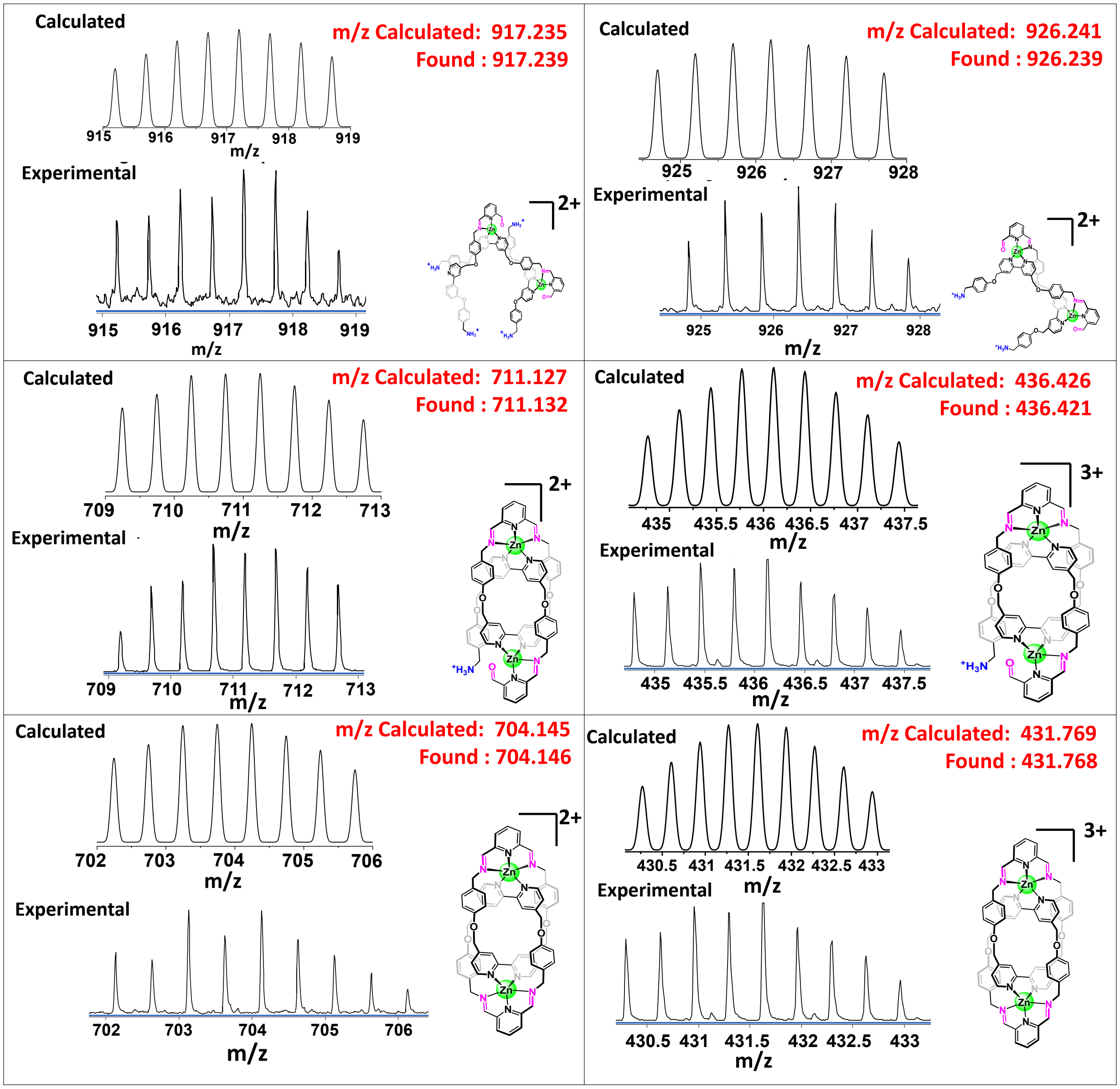
Calculated
m/z Calculated: 917.235
Found : 917.239
915 916 917 918 919
m/z
Experimental
915 916 917 918 919
m/z
2+
Zn
Calculated
m/z Calculated: 926.241
Found : 926.239
925 926 927 928
Experimental
925 926 927 928
m/z
2+
Zn
Calculated
m/z Calculated: 711.127
Found : 711.132
709 710 711 712 713
m/z
Experimental
709 710 711 712 713
m/z
2+
Zn
N
O
^+H_3N
Calculated
m/z Calculated: 436.426
Found : 436.421
435 435.5 436 436.5 437 437.5
m/z
Experimental
435 435.5 436 436.5 437 437.5
m/z
3+
Zn
N
O
^+H_3N
Calculated
m/z Calculated: 704.145
Found : 704.146
702 703 704 705 706
m/z
Experimental
702 703 704 705 706
m/z
2+
Zn
N
O
Calculated
m/z Calculated: 431.769
Found : 431.768
430.5 431 431.5 432 432.5 433
Experimental
m/z
430.5 431 431.5 432 432.5 433
m/z
3+
Zn
N
O

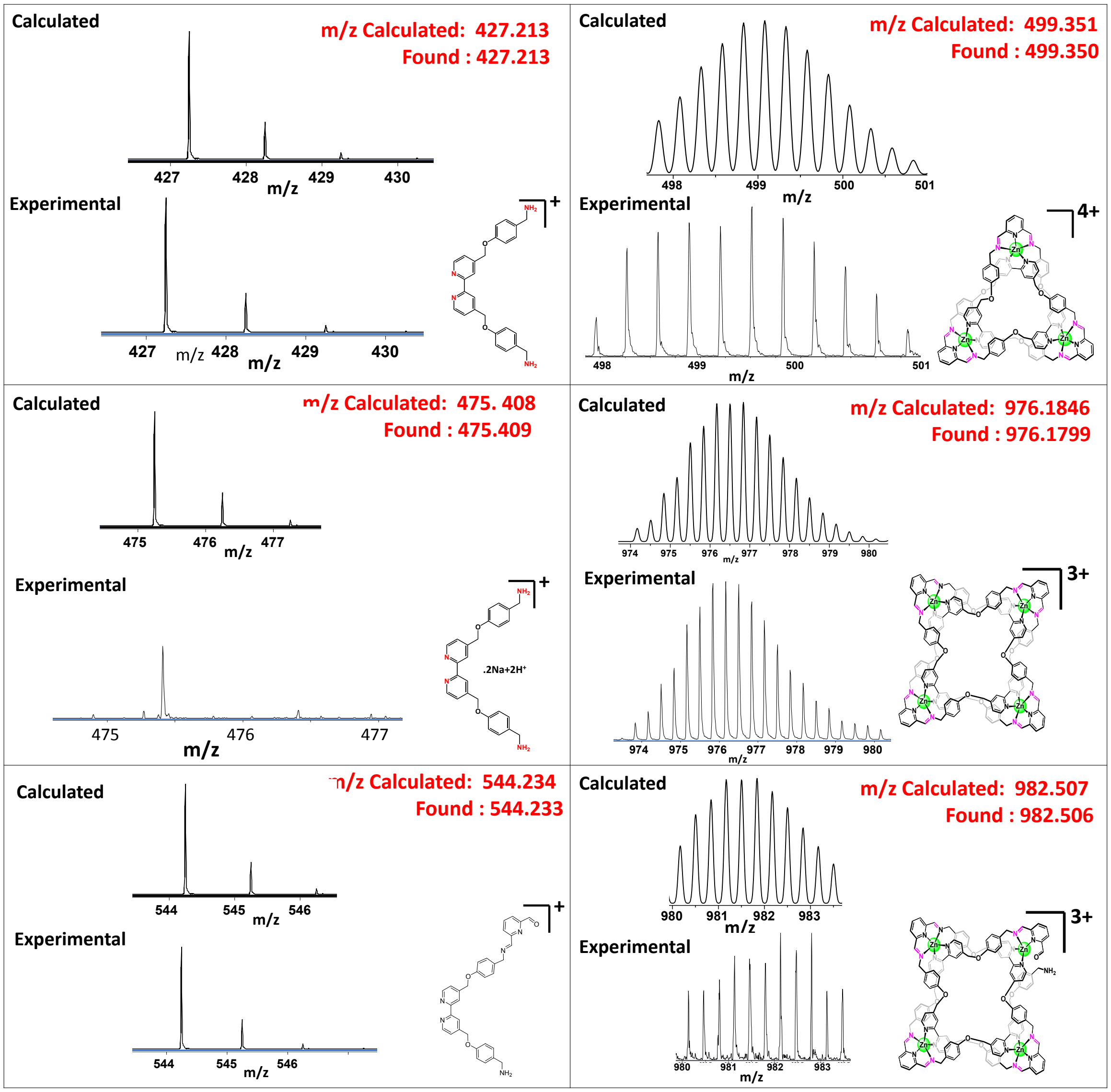

Figure S15b: Expansions of the isotopic distribution patterns of several of the key intermediates (represented in the upper right of each box) identified by HRMS during the transformation of **Cd-TK** into **Zn-[2]C**.

References

1. T. Prakasam, M. Lusi, M. Elhabiri, C. Platas-Iglesias, J.-C. Olsen, Z. Asfari, S. Cianférani-Sanglier, F. Debaene, L. J. Charbonnière and A. Trabolsi, *Angew. Chem. Int. Ed.*, 2013, **52**, 9956-9960.
2. T. Prakasam, R. A. Bilbeisi, M. Lusi, J.-C. Olsen, C. Platas-Iglesias and A. Trabolsi, *Chem. Commun.*, 2016, **52**, 7398-7401.
3. H. E. Gottlieb, V. Kotlyar and A. Nudelman, *The J. Org. Chem*, 1997, **62**, 7512-7515.